Emerging Neural Coincidences in Rats Agranular Medial and Agranular Lateral Cortices During Learning of a Directional Choice Task

by

Bing Cheng

A Thesis Presented in Partial Fulfillment
of the Requirements for the Degree
Master of Science

Approved March 2014 by the
Graduate Supervisory Committee:

Jennie Si, Chair
Junseok Chae
Jae-Sun Seo

ARIZONA STATE UNIVERSITY

May 2014

ABSTRACT

To uncover the neural correlates to go-directed behavior, single unit action potentials are considered fundamental computing units and have been examined by different analytical methodologies under a broad set of hypotheses. Using a behaving rat performing a directional choice learning task, we aim to study changes in rat's cortical neural patterns while he improved his task performance accuracy from chance to 80% or higher. Specifically, simultaneous multi-channel single unit neural recordings from the rat's agranular medial (AGm) and Agranular lateral (AGl) cortices were analyzed using joint peristimulus time histogram (JPSTHs), which effectively unveils firing coincidences in neural action potentials. My results based on data from six rats revealed that coincidences of pair-wise neural action potentials are higher when rats were performing the task than they were not at the learning stage, and this trend abated after the rats learned the task. Another finding is that the coincidences at the learning stage are stronger than that when the rats learned the task especially when they were performing the task. Therefore, this coincidence measure is the highest when the rats were performing the task at the learning stage. This may suggest that neural coincidences play a role in the coordination and communication among populations of neurons engaged in a purposeful act. Additionally, attention and working memory may have contributed to the modulation of neural coincidences during the designed task.

DEDICATION

I dedicate my dissertation work to my family and many friends. A special feeling of gratitude to my loving parents whose words of encouragement and push for tenacity ring in my ears. My wife, Ying, has never left my side and is very special.

I also dedicate this dissertation to my many friends and church family who have supported me throughout the process. I will always appreciate all they have done.

I dedicate this work and give special thanks to my wonderful daughter, Aimee, for being there for me throughout the entire program. She has been my best cheerleader.

ACKNOWLEDGMENTS

I wish to thank my committee members who were more than generous with their expertise and precious time. A special thanks to Dr. Jennie Si, my committee chairman for her countless hours of reflecting, reading, encouraging, and most of all patience throughout the entire process. Special thanks also go to Dr. Junseok Chae and Dr. Jae-Sun Seo for agreeing to serve on my committee. They generously gave their time and expertise to better my work. I thank them for their contribution and their good-natured support.

I would like to acknowledge and thank my school division for allowing me to conduct my research and providing any assistance requested. Special thanks go to the staff of ASU's Department of Animal Care and Technologies (DACT) for their continued support.

Finally I would like to thank the administrators in our school division and fellow students in our lab that assisted me with this project. Their excitement and willingness to provide feedback made the completion of this research an enjoyable experience.

TABLE OF CONTENTS

LIST OF FIGURES

Figure Page

CHAPTER 1

INTRODUTION

Statement of purpose

How neuronal activities encode information is a primary inquiry in the field of neuroscience. For much of the time, the working hypothesis was that information was carried in the spike firing rates. But there remain many open questions about the structure of this coding method. Until now, “How is information coded in neural activity?” is still listed on top of the “10 Unsolved Mysteries of the Brain” (Eagleman, 2007).

The goal of this study is to investigate internal states of the brain via examining the neural coincidences in rats’ AGm and AGl cortex during a directional choice learning process. We hypothesize that neural coincidences are enhanced as a means of providing salient responses for reorganizing the neural network during a directional choice learning process. And the enhanced coincidence abates after learned the task.

Background

A potentially powerful information processing strategy may be within the temporal structures of neuronal spike trains (Abeles, 1991). The concept of neural coincidence, also referred to as neural synchrony, is used to describe temporally synchronous firing of spikes between neurons within several milliseconds. In the early 1970s, it was hypothesized that synchronized interactions between neurons may well occur at the early levels of the sensory path (Milner, 1974), and can be dynamically modulated during different brain states (Von Der Malsburg, 1981). With the introduction of multiple electrode arrays for single unit recording, activities of a neural ensemble became available simultaneously, which led to the first experimental evidence supporting the potential role of neural coincidence as a relational code (Gray and Singer, 1989). Since then, neural coincidence modulation has been extensively investigated (Singer, 1999). These results suggested that neural coincidence is a ubiquitous phenomenon in cortical networks and is likely

to serve a variety of different functions at early levels of sensory processing (Uhlhaas et al., 2009).

The brain is constantly involved in sensory information processing and cognitive information processing. The cognitive function usually refers to higher order brain functions such as attention, working memory, planning, and reasoning, which may be characterized by intrinsic brain states involving information processing for interpreting, responding to and predicting environmental demands (Raichle, 2010). But measuring the internal state of the brain and possibly linking it to neuronal firing mechanism requires a thoughtful experiment design because evaluating the behavioral relevance of intrinsic activity can be a challenging undertaking. Here in this study, we devise a scheme of directional choice learning to reveal the internal states of rats through the phases of him learning to perform a control task. Previous studies have shown modulation of synchronized neural firing during learning processes (Vaadia et al., 1995). Their findings suggested that neurons can self-organize into a functional group for a new task. Tsujimoto (Tsujimoto et al., 2008) revealed that correlated activity could enhance their efficacy in context-dependent goal selection and the transformation of goal choices into action.

The prefrontal cortex has been implicated in planning complex cognitive behavior (Yang and Raine, 2009). The most typical psychological term for functions carried out by the prefrontal cortex area is executive function which relates to abilities to differentiate among conflicting thoughts, determine good and bad, better and best, same and different, future consequences of current activities, working toward a defined goal, prediction of outcomes (Kouneiher et al., 2009). Precentral Cortex, also known as motor area, controls both the preparation of motor movement as well as the execution of movements. Evidence indicates that the classical motor area also has cognitive functions (Hanakawa, 2002). Especially, the supplementary motor area (SMA) has been implicated in actions that are under internal control (Mushiake et al., 1991; Shima and Tanji, 1998). Motor cognition encompasses all the mental processes involved in the planning, preparation, and production of actions, as well as the mental processes involved in anticipating,

predicting, and interpreting the actions (Jackson and Decety, 2004; Tsakiris and Jeannerod, 2008). Motor cortex is also likely involved with different aspects of learning (Hallett, 1995; Debarnot et al., 2011). The frontal cortex of the rat is not well differentiated in comparison to primates (Preuss, 1995; Heidbreder, 2003; Uylings et al., 2003; Seamans et al., 2008). The higher cognitive functions more spread out in prefrontal and precenteral cortex of the rat. Studies of the functions within the relatively undifferentiated frontal cortex of rats can shed light on processing in primate prefrontal cortex. It can also provide a cognitively less complex case, in which the elemental psychological and neural processes can be examined (Brown and Bowman, 2002; Jones, 2002; Kolb and Robbins, 2003).

CHAPTER 2

METHODOLOGY

Animal handling and training procedures

All procedures involving animals were conducted according to the National Guidelines on Animal Experiments and were approved by the Arizona State University Institutional Animal Care and Use Committee. Six male Long Evan rats were used in the study. Rats were handled for 40 minutes daily for about 2 – 4 weeks upon arrival at the age of one month old to make them accustomed to humans. The transition from handling to training began when rats did not squeal or fight when picked up. At that point, rats were placed in a Skinner training chamber, which is similar to the recording chamber (Fig. 1B), with only one cue light and one control paddle to respond to. The cue light inside the chamber indicated to the rat the time to press the control paddles for a sugar pellet reward. A trial was considered failed and thus no sugar pellet rewarded if the rats did not press the control paddle within two seconds of cue presentation.

Recording electrode implantation took place when the rats reached a weight of 390 – 500 grams and were proficient with an accuracy of 90% or higher at pressing the control paddle inside the Skinner training chamber for at least three consecutive days. Once recording began, the rat food was restricted to a daily diet of 12 – 15 grams including the amount of the reward collected during the recording session. The food restricted rats were monitored for their weight to be above 80% of the average weight at their ages.

Surgical procedures

Animal was anesthetized by an intramuscular injection of KXA (0.1 ml/100g of body weight: 0.05 mg/ml Ketamine; 0.005 mg/ml Xylazine; 0.001 mg/ml Acepromazine), followed by injections of 0.2 ml Buprenex (0.03 mg/ml) and 6 ml lactated ringer's solution (3 ml per flank) subcutaneously. The head area between the rat's ears and eyes was shaved. The rat was then mounted on a stereotaxic frame using two ear bars plus the tooth/nose latch. The horizontal plane of the head

was adjusted to be leveled to the stereotaxic support base. The rat's body temperature was maintained between 35°C and 36°C with a heated water blanket. Blood oxygen level and heart rate were monitored throughout the surgery with a pulse oximeter.

The shaved area was sterilized by diluted betadine solution before an incision was made. A patch of skin was removed to clearly expose the skull with coronal suture, sagittal suture, bregma and lambda. Two holes for craniotomy were drilled in the left hemisphere skull of the AGm and AGl cortex, according to the rat brain atlas (Paxinos and Watson, 2007), at 2 mm and 4 mm anterior, respectively, and 2 mm lateral to the bregma. A trepan of 2 mm diameter centered at 3 mm anterior and 2 mm lateral to the bregma was used to cut through the skull. The edge of the cut by the trepan connected the two holes. A rongeur was then used to remove the chiseled bones and to make a 2 mm x 4 mm opening on the skull. Figure 1A illustrates the craniotomy for the electrode array to be placed. Additionally, three anchor holes were drilled between the bregma and the lambda: two in the right hemisphere skull and one in the left, for mounting bone screws which served as a signal ground and also provided fixation to secure the head cap. A 16 channel microwire array (TDT Corporate, Florida) was then lowered slowly into the craniotomy while neural signals were monitored in real time. The target depth was about 1.8 – 2.3 mm from dura aiming for layer-V pyramidal neurons. The final depth was determined by optimal spiking activities on the majority of the recording channels.

The TDT array was made of polyimide-insulated tungsten microwires of 50 um in diameter. The tips were angle cut at 60 degrees and the wires were 5 mm long. The array was configured as a 2 x 8 matrix with 500 um between electrode distance and 375 um row distance. Once the electrode array was put into position, silicon epoxy was used to seal the opening of the skull. After that, an acrylic bump was formed on top of the skull to secure the array onto the bone screws. Finally, 6 ml lactated ringer's solution was injected subcutaneously (3 ml per flank) again, plus a subcutaneous injection of 0.1 ml meloxicam for pain relief. Follow-up injections of meloxicam

were given for three consecutive days after surgery. The rat was given a week or as needed to recover before the food was restricted for experiments.

Electrophysiology

Neural waveforms were recorded through a 16-channel microwire array connected with an omnetics headstage or a Zif-clip headstage (Medusa Connector LP16CH or ZIF-Clip ZC16, TDT Corporate, Florida). Analog waveforms passed through a unity gain preamplifier (Medusa PreAmp RA16PA, TDT Corporate, Florida), which also provided a band-pass filtering (2.2 Hz to 7.5 kHz). The waveforms were digitally sampled at 24414 Hz and then sent over a fiber optic link to a DSP device (RX5/RX7, TDT Corporate, Florida), where they were processed with cross channel denoising in real-time. The stored waveforms were spike sorted offline into single unit action potentials using a multi-scale correlation of wavelet coefficients (MCWC) spike detection algorithm (Yang et al., 2011) followed by a template matching sorting procedure. Events in the behavioral task such as cue on, paddle release, paddle press and food reward were registered simultaneously and time stamped by the TDT system.

Behavioral task

The rat was freely moving inside a Skinner box (Med Associates, Inc., Vermont) when not performing the designed task. The task was self-paced, which was for the rat to associate light cues with control paddles. The chamber was dark with a 0.5 watt infrared light illumination for video recording. Figure 1B is a top view of the recording chamber. When working on the task, the rat faced the front panel of the chamber where five red LED lights were placed. At most one cue light was lit at any given time. The three paddles were used by the rat to complete the association task. The center ready paddle was for the rat to press to signal the start of a new trial. The two control paddles on each side of the center paddle were for controlling the movement of the light position. The food pellet dispenser was located under the center paddle for rewarding the rat.

The goal of the task was to move the light position to the center by pressing the control paddles and remain there for one second. Figure 1C is an example of a complete trial of the behavioral task. The rat was not able to start a new trial until a lapse of eight seconds for previously successful trials and fifteen seconds for previously failed trials, respectively. Upon pressing of the center paddle by the rat to start a new trial, one of the five cue lights was lit. Two seconds later, both control paddles were released. A right paddle press moved the light to the left by one light position and similarly for the left side. The rat was naïve initially and he learned the task by trial and error. If he managed to keep the light to remain in the center position for one second, he would be rewarded with food pellets. If the rat did not respond by pressing any paddle within the time allowance or if the light moved out of range, the trial was deemed a failure.

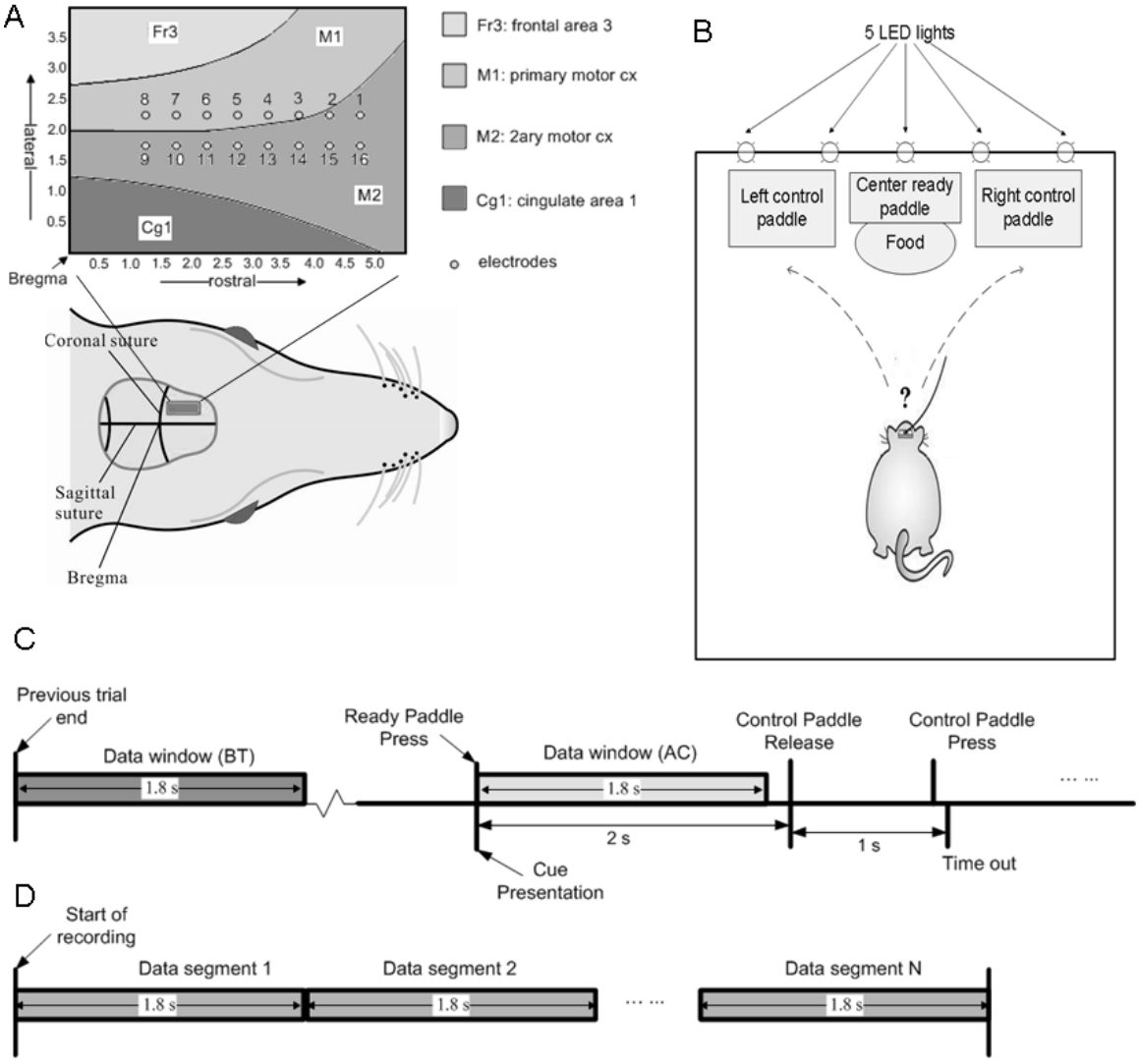

Figure 1: Experimental setup. A, Implant site. a 16-channel array was placed in the frontal area of the rat with the center at 3 mm anterior and 2 mm lateral from the bregma. It covers AGm and AGl areas. B, Top view of the recording chamber. The rat pressed the center ready paddle to signal the start of a new trial. As one of the cue lights appeared, the rat had to make a decision of pressing either the left or right paddle to control the movement of the light. C, Task timeline. Two data windows were used in the analysis.

The first 1.8 s window was from the end of the previously failed trials, which located between two consecutive trials (abbreviated as BT, shaded in dark grey). The second 1.8 s window was right after cue on (abbreviated as AC, shaded in light grey). Upon center paddle press, one light cue was lit immediately. Two seconds from cue on, both left and right control paddles were released for the rat to choose from within one second. Otherwise, the trial was timed out as failed. If the rat moved the light out of range, the trial was also considered a failure. D, In addition to data recorded while the six rats performed the directional choice learning control task, for rats Q10 and G11, we also recorded them while they were not performing any task but simply freely moving about in the recording chamber. These recordings were divided into consecutive segments of 1.8 s long. A total number of N segments were used in analysis where N is the number of successful trials the rats performed on the same day.

Data analysis

Neural waveforms of six rats (W09, A09, B10, L10, Q10 and G11) were recorded while they performed the directional choice learning task. The waveforms were offline sorted as described previously. For rats W09, A09 and B10, four well isolated neurons were used in the analysis while for rats L10, Q10 and G11, three were used. In this study, two sets of data were considered. The first set included data from the four rats (W09, A09, L10 and B10). The second set included data from the other two rats (Q10 and G11). The two sets of data are detailed as follows.

For the first set of data from the four rats W09, A09, L10 and B10, the behavioral states were divided into two stages according to the rats' behavioral accuracies. The learning stage (LG) was associated with the rats improving their task performance accuracies over time until reaching a percentage accuracy of 80% or higher, while the learned stage (LD) was designated as the period after learning (Fig. 2).

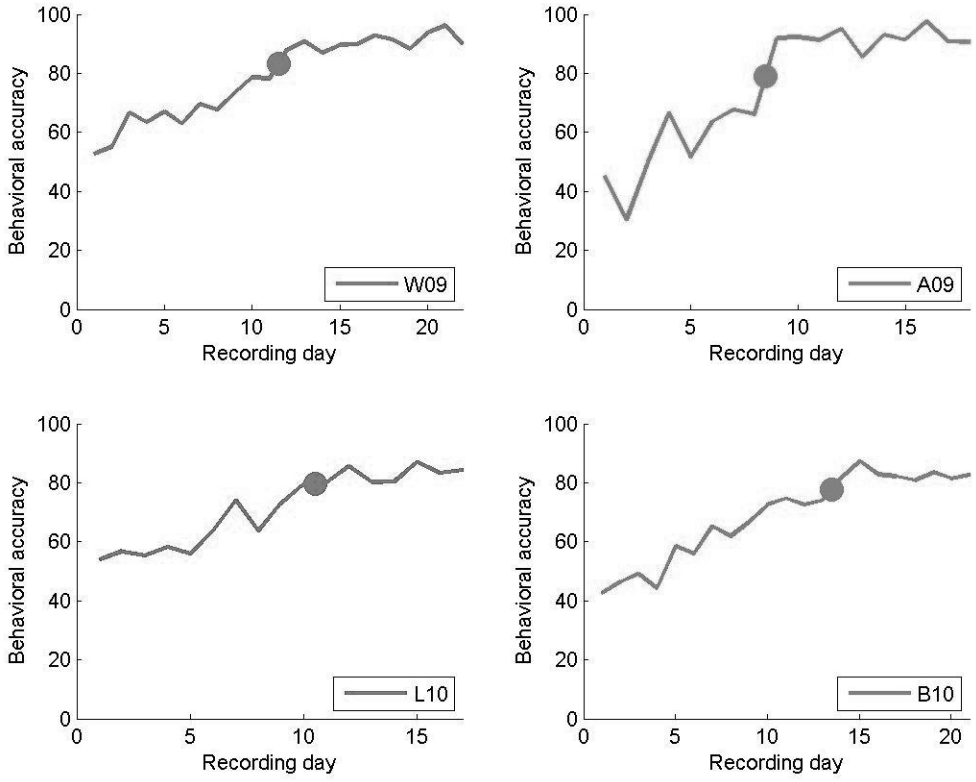

Figure 2: Behavioral learning curves for four rats W09, A09, L10 and B10. The solid dots on the learning curve indicate when the rats reached a performance accuracy of 80% or higher. The parts of the learning curves to the left of the solid dots correspond with the learning stage (abbreviated as LG) while those to the right, the learned stage (abbreviated as LD).

Also for those four rats, neural spike data were examined in two windows (Fig. 1C). The first was the one between two consecutive trials (BT). Only previously failed trials were used since the time between trials in this case was longer than for successful trials. Data from this window served as

control in the study. The second window was the one after cue onset (AC) for all correct behavioral trials. This is the period of time implied in learning the meaning of the cue and planning appropriate actions by rats in order to receive a food reward at the end of each trial. We were expecting to find elevated synchronous spike firing in this window during the learning process.

In the second data set, rats Q10 and G11 were not able to learn the task before losing their neural signals. Therefore only data during the learning stage were used in the analysis. But we recorded their neural activities while they freely moved about without task performance (referred to as resting stage or RG). That was done immediately after their regular recording of task performance. The recorded neural data during the resting stage were divided into non-overlapping segments as shown in figure 1D, which were used as control in the study. The number of the segments and the length of each segment were selected to be the same as the number of successful task trials and the data window length in each trial, respectively for analysis.

We evaluated the cross correlation over time between neuron pairs using joint peristimulus time histogram (JPSTH), which is a 2-dimensional histogram for each neuron pair that displays the correlated activities of two spike trains relative to behavioral events. It is a widely used technique in the analysis of interactions among neurons in the neuroscience community (Aertsen et al., 1989; Sillito et al., 1994; Havenith et al., 2009). In the present experiment, we used a bin size of 1 ms to study correlated firing of two spike trains where usually each bin value was either one or zero, corresponding to the existence of a spike or otherwise, respectively.

In the following analysis, one pair of neurons (*x* and *y*) was studied at a time. The value of each bin was represented by $N_x^{(k)}(i)$ or $N_y^{(k)}(i)$ for neuron *x* and *y*, respectively, as shown in figure 3A where *k* was the trial number and *i* was the bin number. The JPSTH can then be represented

by a matrix with spike trains of neuron *x* on the horizontal axis and *y* on the vertical. Each component in the matrix represented a coincidence value $N_x^{(k)}(i) * N_y^{(k)}(j)$ as shown in figure 3B.

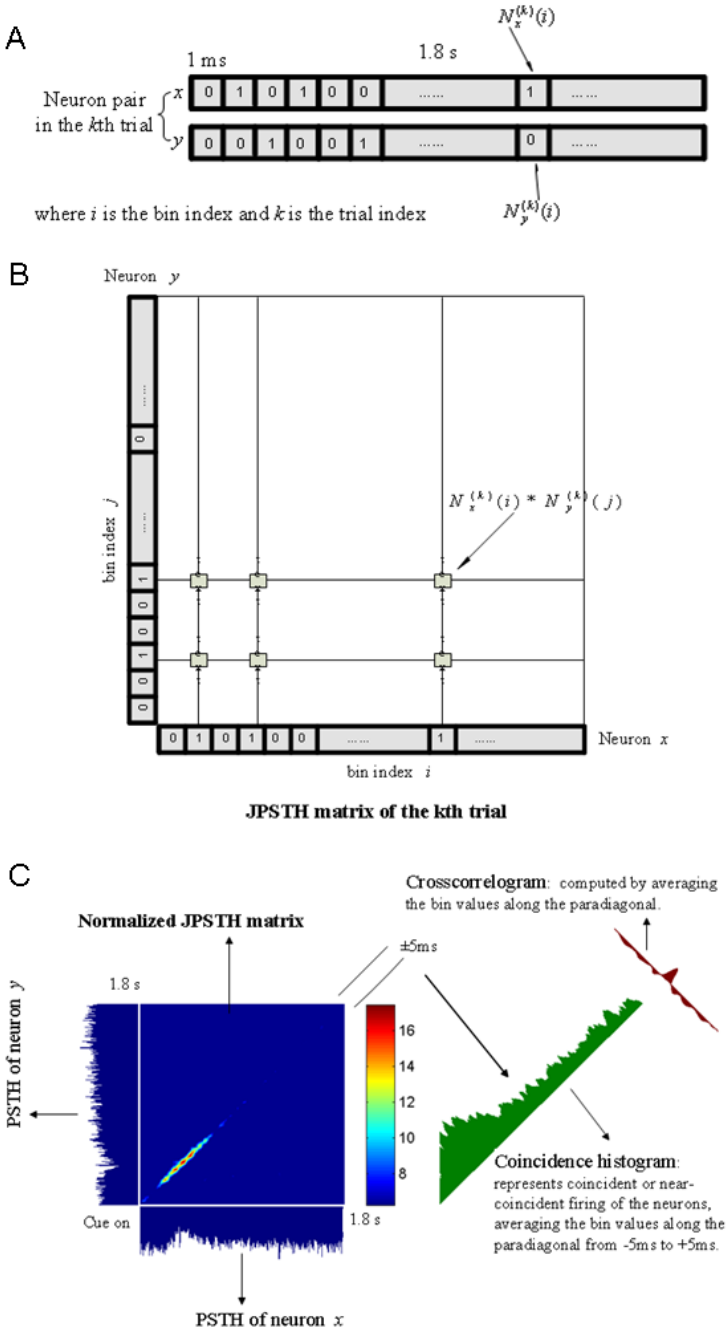

Figure 3: Creating the JPSTH: A, Quantitate two spike trains into 1 ms bins. B, Put them into a matrix to obtain a JPSTH for each trial. C, The normalized JPSTH matrix is computed according to equation (2) and placed on the left side of the panel; the coincidence histogram is to the right of the matrix while the crosscorrelogram is at a right angle to the coincidence histogram.

To obtain a raw JPSTH, each element $J(i,j)$ in the matrix was averaged over all trials as shown in equation (1),

$$J(i,j) = E[N_x^{(k)}(i) * N_y^{(k)}(j)] = \frac{1}{M}\sum_{k=1}^{M} N_x^{(k)}(i) * N_y^{(k)}(j) \quad (1)$$

The firing rates of the two neurons had influence over the raw JPSTH and the influence should be removed in order to evaluate the changes in coincidence. The raw JPSTH was normalized by subtracting the multiplication of mean firing rates of both neurons and then scaled by the covariance between the two neurons, according to equation (2),

$$\hat{J}(i,j) = \frac{J(i,j) - P_x(i) * P_y(j)}{S(i,j)}, \quad (2)$$

where

$$P_x(i) = E[N_x^{(k)}(i)] = \frac{1}{M}\sum_{k=1}^{M} N_x^{(k)}(i),$$

$$P_y(i) = E[N_y^{(k)}(i)] = \frac{1}{M}\sum_{k=1}^{M} N_y^{(k)}(i),$$

and

$$S(i,j) = \sqrt{\{E[N_x^k(i) - P_x(i)]^2\} * \{E[N_y^k(j) - P_y(j)]^2\}}.$$

An illustration of the above computation is shown in figure 3C. Normalized JPSTH matrix is shown at the left while the coincidence histogram is at the right. It represented coincident firing between two neurons within close proximity in time of millisecond range. A narrow band of ±5 ms (figure 3C) was used to compute the coincidence histogram according to the discussions in

(Larkum et al., 1999) where the authors showed that layer-V pyramidal neurons could detect dendritic coincidence occurred within a 10 ms window. The crosscorrelogram presented at a right angle to the coincidence histogram was computed by summing the bins along the para-diagonal direction. We also computed peristimulus time histograms (PSTHs) of neurons x and y and put them along the horizontal and the vertical axes, respectively. A coincidence measurement is defined by averaging the bin values of the coincidence histograms. Equivalently it can also be computed by averaging over all elements along the ±5 ms para-diagonal band of the normalized JPSTH matrix or averaging bin values from -5 ms to +5 ms of the crosscorrelogram.

CHAPTER 3

EXPERIMENT RESULTS

Spike sorting

Waveforms of 6 rats were recorded while rats performed the directional choice learning task. A one-second segment of the original raw waveform from rat W09 is shown in figure 4A. Before spike sorting, raw waveforms were band filtered from 300Hz to 3000Hz to remove 60Hz harmonics, low frequency fluctuation and high frequency noise. The signal-to-noise ratio (SNR) after filtering is about 10dB. The multiple correlation of wavelet coefficient (MCWC) spike detection algorithm (Yang et al., 2011) was employed for offline spike detection. First, a set of spike templates were created using the MCWC as shown in figure 4B. The neural waveforms were then spike detected and sorted using the templates generated with examples of sorted spikes shown in figure 4C. Finally, the sorted spikes from the previous steps were manually inspected and confirmed if they meet the following criteria: 1) good template shape, 2) small variance from the template, and 3) reasonable firing rate. In this example, the spikes in the top left panel of figure 4C were selected as action potentials of a neuron recorded from one of the sixteen electrodes.

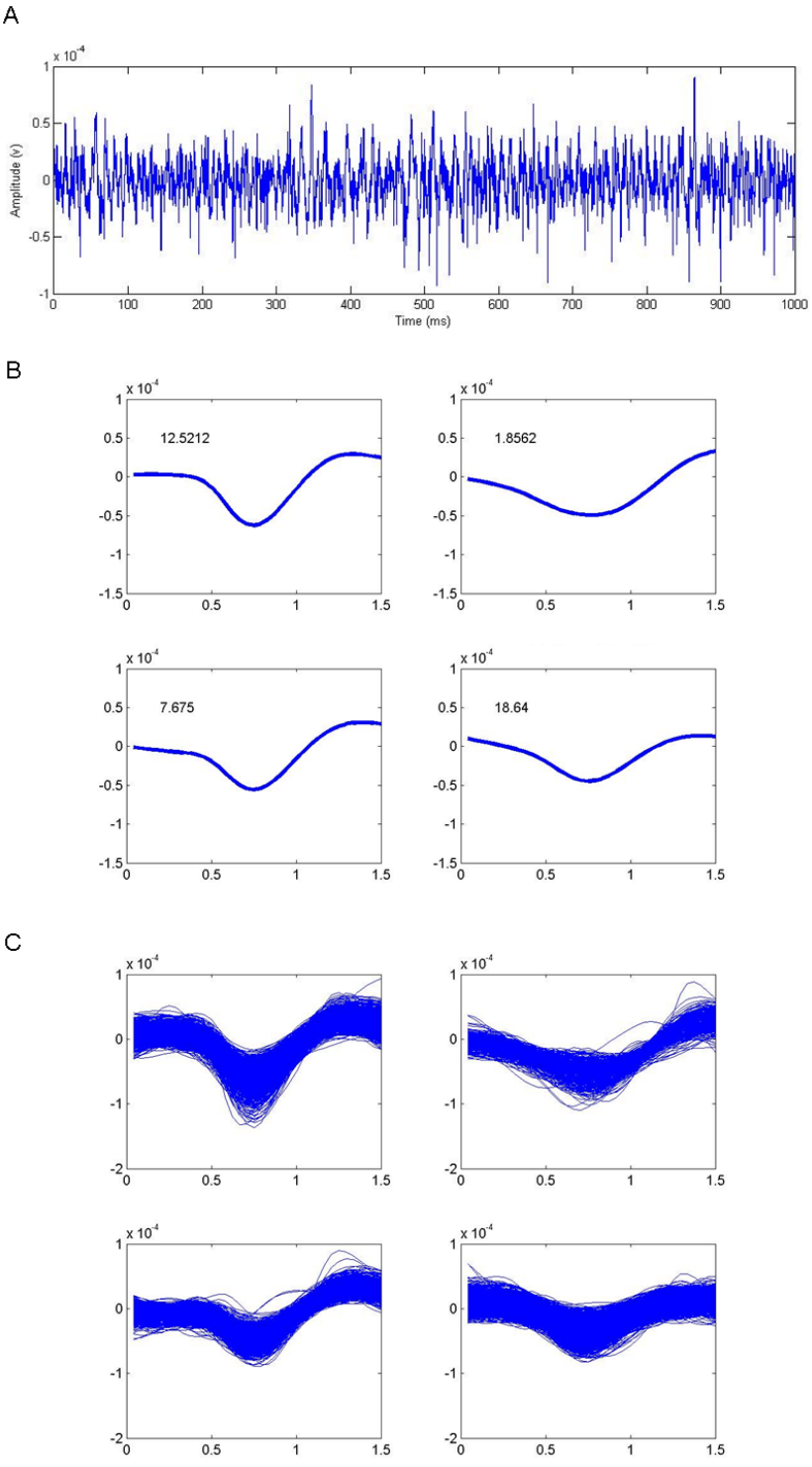

Figure 4: Neural waveform and spike sorting from a channel of rat W09: A, A segment of recorded neural waveform of one second long, which was band filtered from 300Hz to 3000Hz. B,

Templates of clusters of neural spikes using the MCWC spike detection. The number inside each panel depicts the firing rate of the cluster. The y-axis is the waveform amplitude in volt and the x-axis is time in millisecond. C, Spike candidates detected in each cluster. Same coordinate convention as in B. The spikes in the top left panel were considered as the action potentials from that channel.

Results from the first data set

The first set of results is based on analysis of data from four rats W09, A09, L10 and B10. We compared the coincidence measurement computed from the window of after cue on (AC) and the window of between trials (BT) (Fig. 1C), from data at the learning stage (LG) and the learned stage (LD) (Fig. 2). As an example, one pair of neurons of rat W09 between the learning stage and the learned stage is shown in figure 5. Figure 5A includes example raster plots for the learning stage (left panel) and for the learned stage (right panel). The green dots represent spikes of one neuron; the blue dots represent spikes of another neuron; and the red squares depict events in which the two neurons fire spikes within a small time window (10 ms). We can see clearly that the two neurons exhibited a higher coincidence of firing together at the learning stage than the learned stage. Figure 5B shows the same trend using normalized JPSTH. The region around the main diagonal line in the normalized JPSTHs represents events of two neurons firing within a close time window. The left panel, which is for the learning stage, has more coincidental spiking events than that in the right panel, which is for the learned stage.

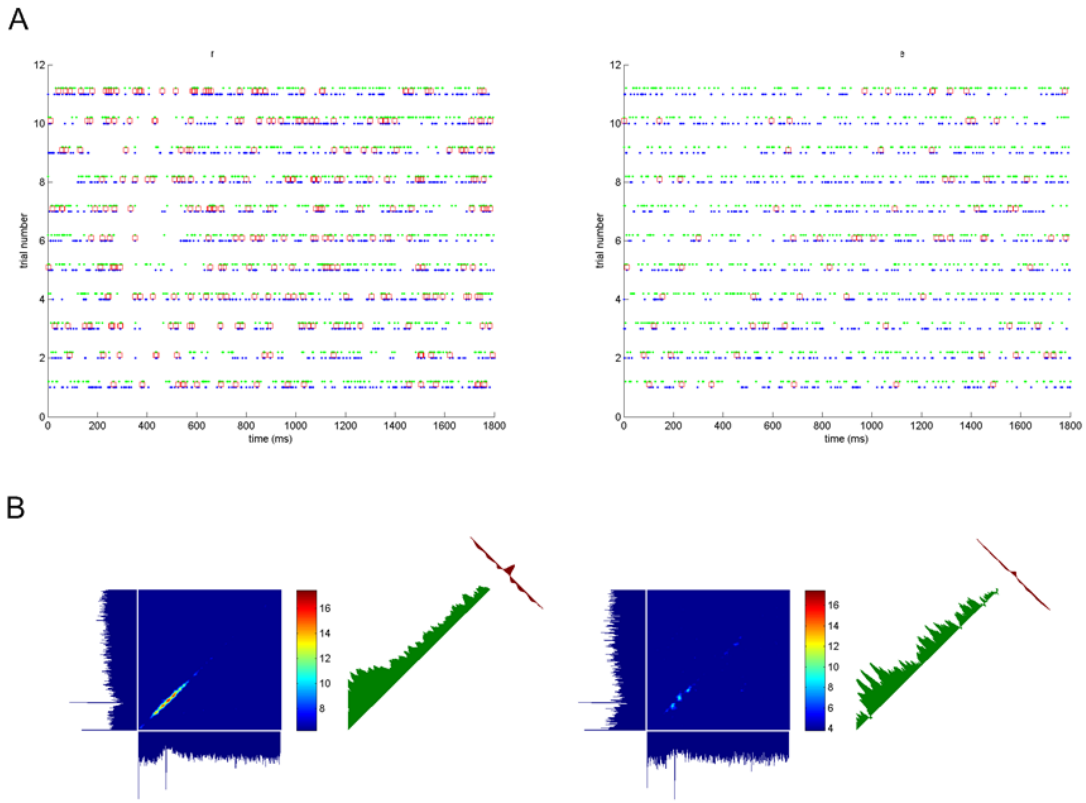

Figure 5: Comparison of neural activities during the learning stage (left column) and the learned stage (right column) for a pair of neurons of rat W09. A, Example raster files of a pair of neurons. The spikes of the paired neurons are shown as green and blue dots, respectively. The red squares denote the coincidence events that two neurons fire spikes within a 10 ms window. B, Normalized JPSTH matrix for the same pair of neurons. The coincident activities appear focused on the main diagonal of the matrix.

The normalized JPSTHs of the other three rats (A09, L10 and B10) are shown in figure 6. The left column is for the learning stage and the right column for the learned stage. Similar to the observation from figure 5 for rat W09, for rats A09, L10 and B10, we also see that neuron pairs exhibited a higher level of coincidence firing at the learning stage than the learned stage.

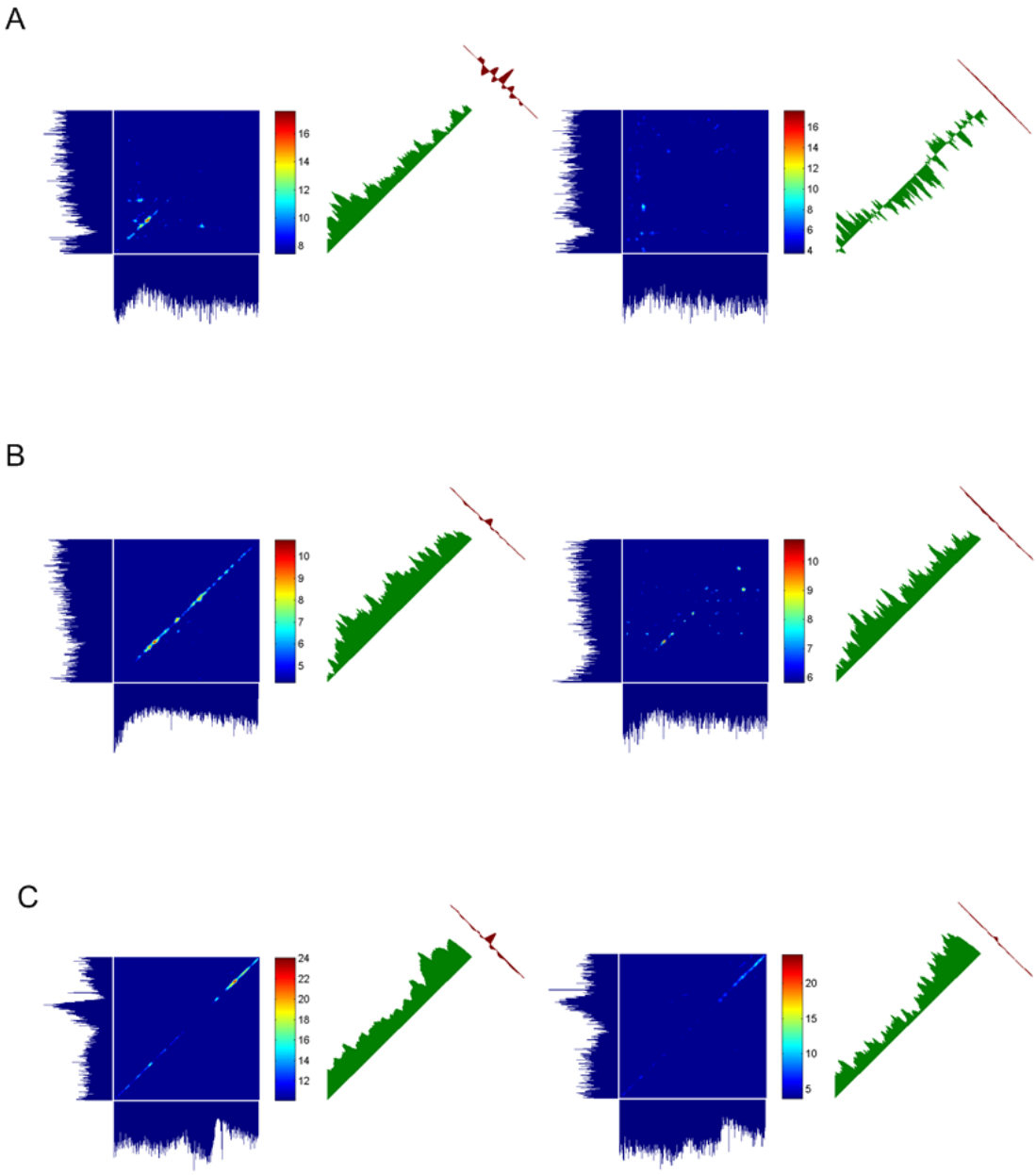

Figure 6: Normalized JPSTH matrices of a neuron pair for rat A09 (A), L10 (B) and B10 (C). The left column has results for the learning stage, the right column for the learned stage.

Next, data were analyzed for each pair of the recorded neurons and for each rat. To account for behavioral features, neural data were organized accordingly into the following four groups:

1. AC_LG: the window of after cue on (AC) at the learning stage (LG);
2. AC_LD: the window of after cue on (AC) at the learned stage (LD);
3. BT_LG: the window of between trials (BT) at the learning stage (LG);
4. BT_LD: the window of between trials (BT) at the learned stage (LD).

The coincidence measurements were then computed for each pair of the recorded neurons within each of the four groups. Specifically, we have 21 pairs of data for comparison in each of the above four groups: 6 pairs for W09; 6 pairs for A09; 3 pairs for L10; and 6 pairs for B10. In all comparisons conducted using this first data set from the four rats, the coincidence measurements computed from between trials (BT) serve as baselines in my analysis.

A summary of the coincidence measurements using normalized JPSTHs resulted from the above four groups for all four rats is shown in figure 7. It is apparent that the coincidence measurement is higher at the learning stage than that at the learned stage, which is especially so in the window after cue on. At the learning stage, the coincidence measurement in the window after cue on is higher than that in the window of between trials. But at the learned stage, there is no significant difference in coincidence measurement between the AC window and the BT window.

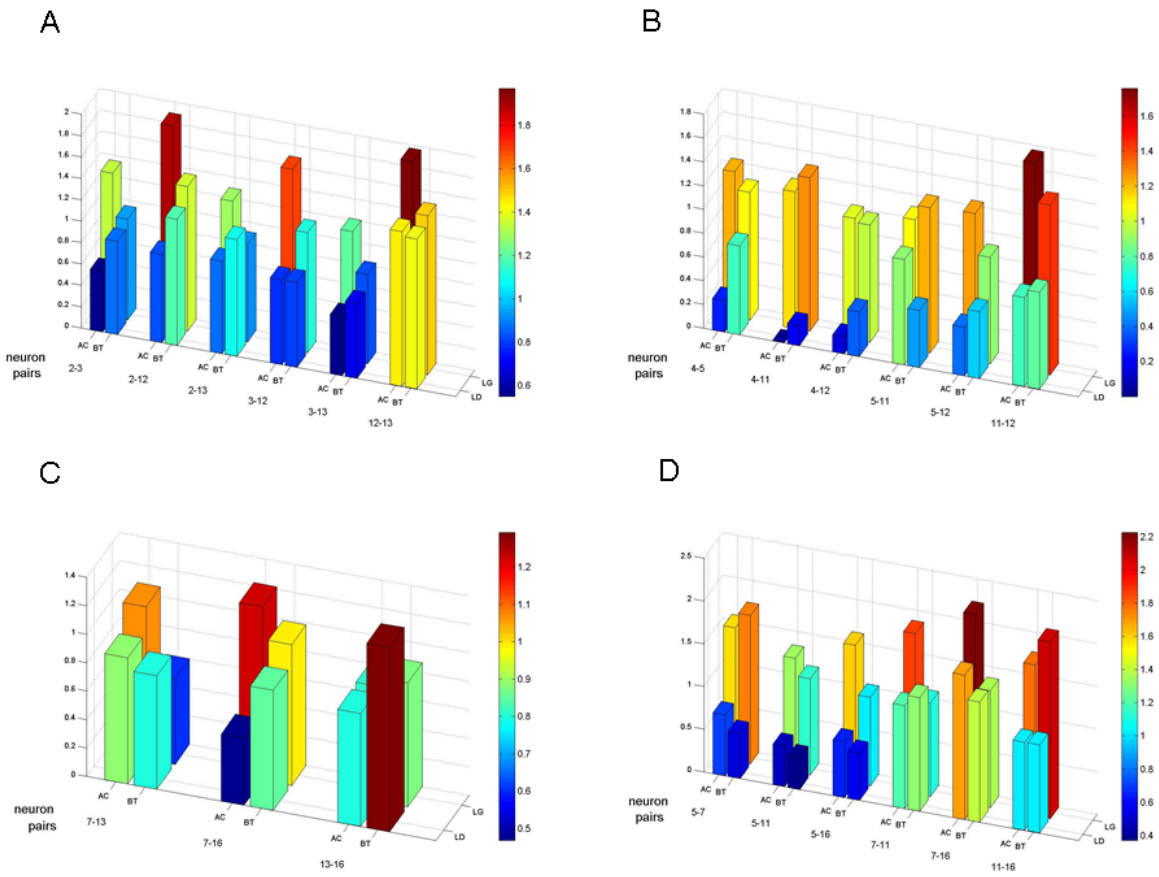

Figure 7: Coincidence comparison for rat W09 (A), rat A09 (B), rat L10 (C) and rat B10 (D). AC: the window after cue on. BT: the window between trials. LG: the learning stage. LD: the learned stage. The y-axis represents the values of the coincidence measurements. Four cases are grouped into one cluster for comparison. It is apparent that the coincidence measurement is higher at the learning stage (LG: the bars in the back row) than that at the learned stage (LD: the bars in the front row). This is especially so for after cue on (AC: left columns of each group). At the learning stage (LG), the coincidence measurement for after cue on (AC: the bars in the back left of each group) is higher than that between trials (BT: the bars in the back right of each group). But at the learned stage (LD: the bars in the front row), there is no statistically significant difference in coincidence measurement between AC and BT.

To provide a quantitative evaluation of the statistical significance of the results obtained using the coincidence measurements as summarized in figure 7, one way ANOVA was employed (Matlab

Statistics Toolbox, MathWorks Inc, MA). It showed significant differences in coincidence measurements among the four groups (H = 1; alpha = 0.05; F[3,83] = 16.5980; p = 1.7830e-008). Post hoc analysis was conducted using paired student tests. Six conditions of paired comparisons from the four groups were carried out, but the two conditions of (AC_LG vs BT_LD) and (AC_LD vs BT_LG) are not relevant and thus not included here since they do not have a common basis for comparison. We therefore performed the student tests under the following four conditions with respective statistical results presented below.

1. AC_LG vs BT_LG (H = 1; alpha = 0.05; t[1,20] = 4.0609; p = 6.1018e-004);
2. AC_LD vs BT_LD (H = 0; alpha = 0.05; t[1,20] = -1.7606; p = 0.0936);
3. AC_LG vs AC_LD (H = 1; alpha = 0.05; t[1,20] = -10.7716; p = 8.9373e-010);
4. BT_LG vs BT_LD (H = 1; alpha = 0.05; t[1,20] = -3.3846; p = 0.0029).

The coincidence measurement in the window of after cue on (AC) increased significantly compared to the control, which is the window of between trials (BT), during the learning stage (the first condition). But there is no statistically significant difference in the two windows during the learned stage (the second condition). The coincidence measurement showed significant difference between the learning stage (LG) and the learned stage (LD) in the window of after cue on (the third condition). This tendency also preserved in the window of between trials (BT), but with a much larger p value and thus the difference is not as pronounced (the forth condition).

Based on the above analysis, we examined the two conditions (AC_LG vs BT_LG, AC_LG vs AC_LD), which showed strong statistical significances in further detail. In figure 8A and figure 8B, the coincidence measurements for each neuron pair and each rat are plotted for each of the two conditions. Again, sample-wise results confirmed my hypothesis. To summarize, we find that the coincidence measurement in the window of after cue on at the learning stage (AC_LG) is the highest among the four groups (Fig. 8C).

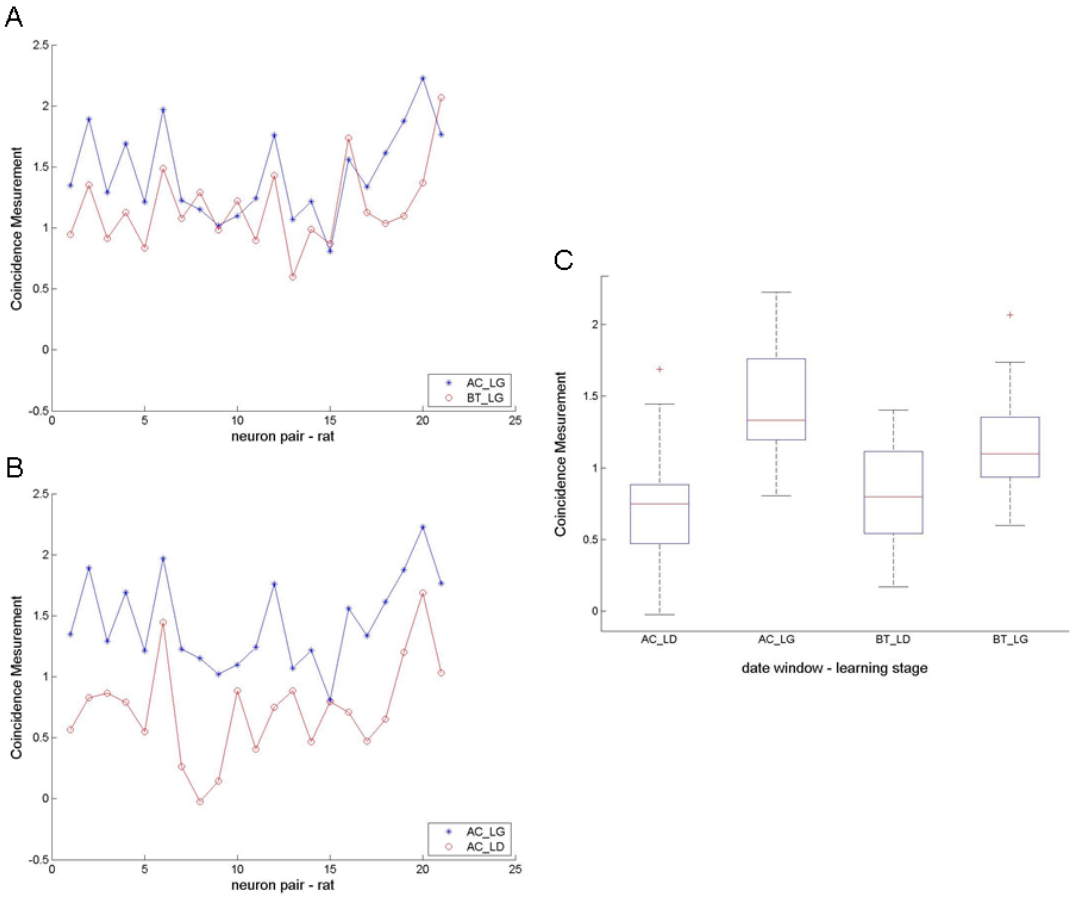

Figure 8: A, Comparison of the coincidence measurement in the AC window and the BT window at the LG stage. B, Same comparison as at the LG stage with the LD stage in the AC window. C, Side by side comparison of the coincidence measurement in different data windows (Fig. 1C) and at different learning stages (Fig. 2). The line inside the box bar is the median, the two ends of the box are the 25th and 75th percentile, respectively, and the whiskers extend to the most extreme data points. The outliers are symbolized by the crosses. It is clear that the coincidence measurement in the after cue on window at the learning stage (AC_LG) is the highest among the four groups.

Results from the second data set

Rats Q10 and G11 did not completely master the directional choice learning task during their recording periods. They only provided data for the learning stage (LG). Therefore neural recordings from these rats during the resting stage (RG) were used as control for comparisons. All other conditions remained the same. We computed the normalized JPSTHs for the learning stage (LG) and the resting stage (RG) of rats Q10 and G11. Figure 9A and 9D are the neuron pair firing coincidence measurement values for the learning stage of Q10 and G11, respectively. Prominent display of strong correlation can be seen along the para-diagonal line in both rats. The results of the resting stage of Q10 and G11 are shown in figure 9B and 9E, respectively. Some activities, but much weaker than that at the learning stage, were noticed along the para-diagonal line. It is consistent with the observations based on the other four rats that the coincidence measurements were higher in the window of after cue on (learning) than that in the window of between trials (resting).

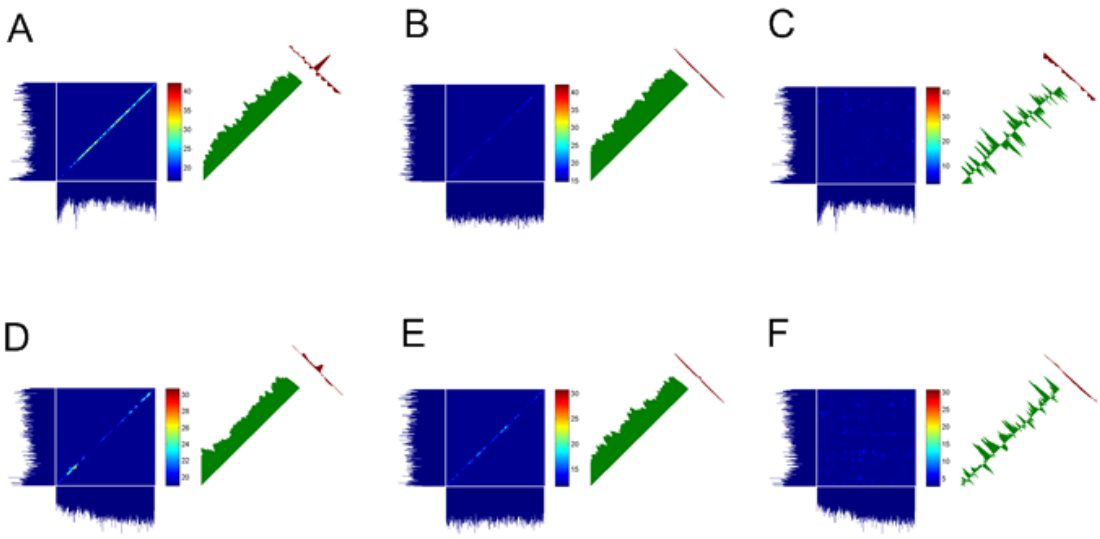

Figure 9: The normalized JPSTHs for rat Q10 (top row) and rat G11 (bottom row). A and D, Learning stage. B and E, Resting stage. C and F, Shuffled data.

We also shuffled the neural data to eliminate any potential temporal relationship between two neurons. The normalized JPSTHs of shuffled data are shown in figure 9C and 9F for Q10 and G11, respectively. Clearly no significant presence of any coincidence pattern can be observed. The comparison of coincidence histogram based on data at the learning stage, the resting stage and the shuffled data is shown in figure 10. The left column includes results from rat Q10 and the right column from rat G11. Each panel corresponds to a pair of neurons. The coincidence histogram of shuffled data is about zero as expected. The coincidence histogram at the learning stage is higher than that at the resting stage. We computed the coincidence measurement which is defined the same way as in the previous four rats and show them in figures 11A and 11C for Q10 and G11, respectively. The coincidence measurement at the learning stage is higher than that at the resting stage ($H = 1$; alpha = 0.05; $t[1,5] = 3.0006$; $p = 0.0301$). One more interesting observation from figure 10 is that the coincidence histogram at the learning stage is more dynamic with higher mean values and higher standard deviations. We computed the variance of the smoothed coincidence histogram (Fig. 10) and compared both learning and resting stages as shown in figures 11B and 11D for Q10 and G11, respectively. The paired student test also shows significant differences in these variances ($H = 1$; alpha = 0.05; $t[1,5] = 3.3989$; $p = 0.0193$). This may suggest a rather dynamic reorganization process in the neural ensemble at the learning stage.

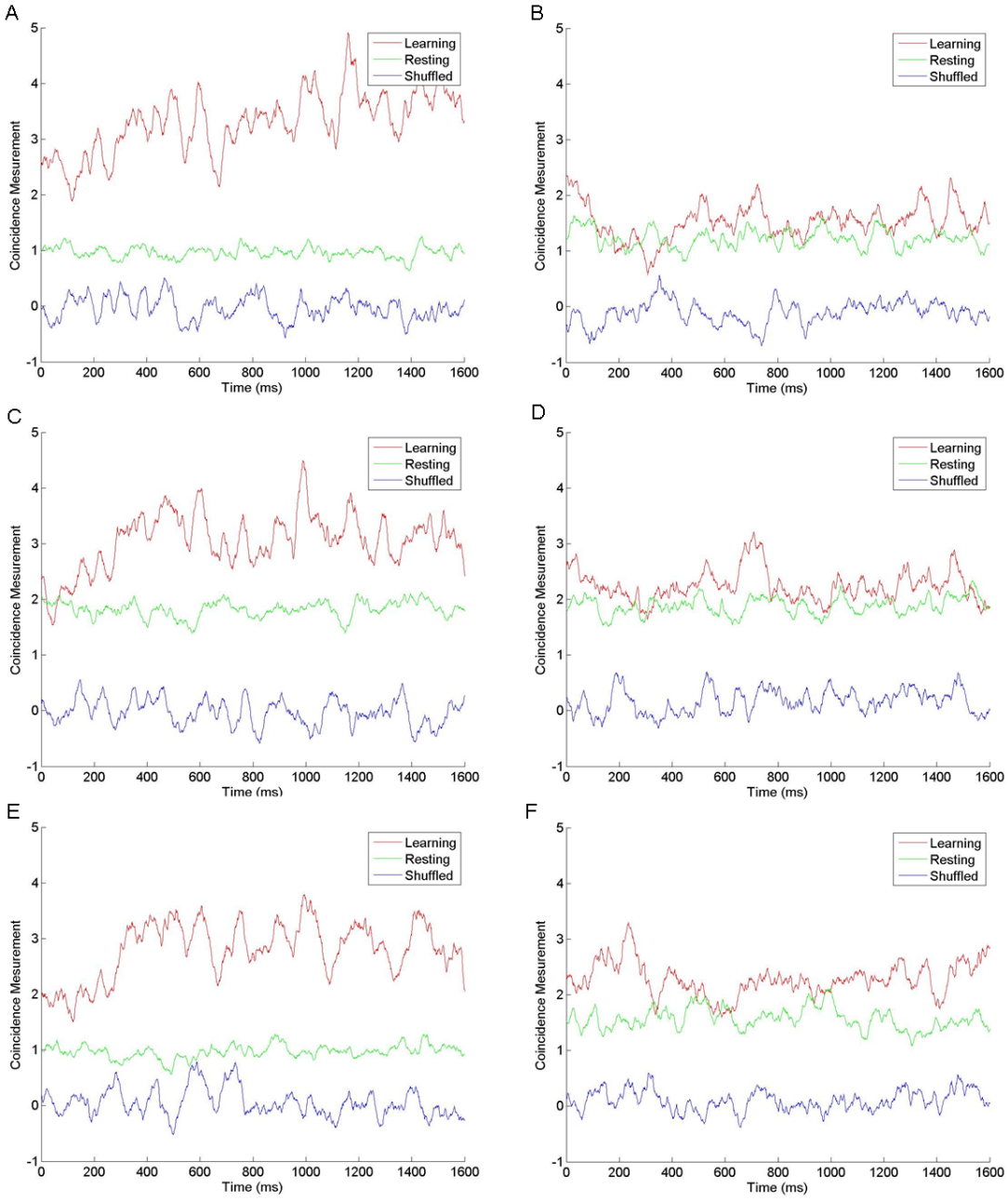

Figure 10: Coincidence histograms. The left column is for rat Q10 while the right column is for rat G11. Each panel is the result from a pair of neurons.

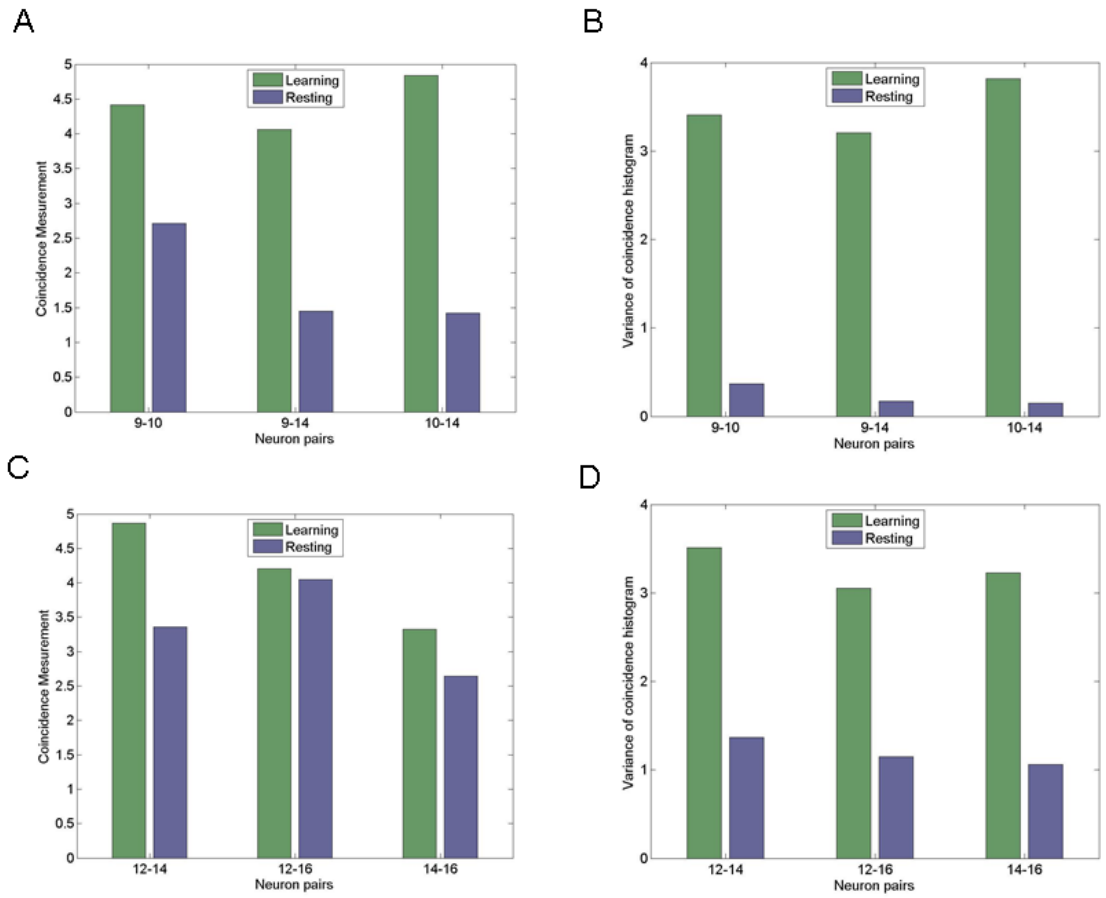

Figure 11: Neuron activity for rat Q10 and G11. Comparison of the coincidence measurements at the learning stage and the resting stage (A, C). Comparison of variances of the coincidence histograms at the learning stage and the resting stage (B, D). The results of rat Q10 are shown in the top row while that of rat G11 in the bottom row.

CHAPTER 4

DISCUSSION

Correlation based coding

Identifying elementary symbols and characterizing the messages that the symbols represent are important steps toward understanding the neural code. Several possible elementary symbols have been proposed and considered, implicitly or explicitly. Correlations between spike trains are among the first to be considered as neural coding symbols. Two possible computations of neuronal correlations have been used. The first is based on temporal correlation of a single neuron between two different time segments (Victor and Purpura, 1996; Brenner et al., 2000). The second is cross correlation between two isolated neurons, which can be both during the same time segment or different (Averbeck et al., 2006; Kilavik et al., 2009; Aldworth et al., 2011).

Complementary to the traditional rate code, evidence shows that the correlation code can provide additional information (Grün, 2009). In an in-vitro study, Rocha (De La Rocha et al., 2007) recorded layer-V neurons in slices from auditory and somatosensory cortices of young mice. Correlated spike trains were evoked by stimulating with Gaussian currents. The correlation coefficient increased with the discharging rate of the neurons while the input correlation was unchanged. In another in-vitro study, Pillow (Pillow et al., 2008) suggested that correlated activities could convey more information about visual stimuli. Di Lorenzo (Di Lorenzo et al., 2009) demonstrated that spike timing correlation of broadly tuned neurons played an important role in the representation of taste stimuli. Information theory (Shannon, 1948) has achieved great success in many fields. Recent applications of information theory to the analysis of spike trains have led to a better understanding of neural networks. Spike correlations may be considered a means of increased information content of the encoded signal (Rolls and Treves, 1998; Abbott and Dayan, 1999).

It is necessary to reliably identify same neuron spike trains across days. People use features of recorded waveforms, such as amplitudes, shapes, energy and inter spike intervals, as well as correlation measures to inspect if two units from different recording sessions may be the same neuron. The issue can be complicated by decaying in waveform amplitudes and changing shapes of spikes recorded on the same electrode. Similarly, inter spike intervals may also change at different recording session.

In my analysis, in addition to careful spike sorting using our advanced spike sorting algorithm, the M-Sorter (Yuan et al., 2012), we also manually examined the waveform features to verify same neurons. Even though my results required individually sorted spikes, my conclusion is based on a collective account of multiple neurons, which are considered stationary during one recording session.

Intrinsic states relate to synchronized spike firing

In most published results, measurable brain responses to controlled stimuli have been used and proven effective in increasing our understanding of the underlying neural circuits, and thus the respective brain function. In this reflexive view on the brain function, the nervous system would be seen to remain inactive until stimulated by sensory inputs, at which time it would process the sensory information and generate an appropriate output. Concurrently, recent developments in neuroscience have emphasized the internal function of neuronal circuits beyond simple responses to the external inputs. Studying the intrinsic activities might lead to important discoveries of higher order brain function. But evaluating the behavioral relevance of intrinsic brain activities can be an elusive undertaking (Yuste et al., 2005; Raichle, 2010). To make the problem tractable and specific, we designed a learning task of conditional sensory-motor association. The concept of sensory-motor association was defined in (Sanes and Donoghue, 2000). In this study, we examined the relationship between the neural coincidences of two spike trains and the intrinsic states of the rats when they performed the directional choice learning task. My designed task aimed at eliciting intrinsic neural activities and consequently an internal neural

state representation as a response to how the brain would interpret the sensory cues. Throughout the learning process, the extrinsic condition did not change in the experiments, but the rats' internal states evolved with their learning of the task. The modulations in rats' neural activities represented such changes in internal states. It was noted that associative learning is always accompanied with an increase in "mental effort" or arousal (Kahneman, 1973). Unfortunately, it is difficult to directly address questions regarding mental effort and arousal state especially by using animal models, in part because these concepts are often used too generally to be properly operationalized (Barch et al., 1997). However, it is possible that specific processes, such as attentional effort and working memory load, can be associated with a behavioral performance measure at different learning stages. Further discussions on the relationship of neuronal synchrony and the intrinsic activity such as attention and working memory can be found in a review paper in (Wang, 2010).

Other groups have also published data to address the relationship between synchronized firing and intrinsic brain activities. Fries (Fries et al., 1997) showed that synchronization of individual action potentials among neurons in V1 could be modulated from one perceptual condition to another. In a delayed-response hand movement task, Riehle (Riehle, 1997) found that neural synchrony in motor cortical neurons increased while firing rates remained the same during the planning period which corresponded to internal "expectation" events. Sakamoto (Sakamoto et al., 2008) showed that synchronized firing increased during a transitional stage when the neuronal activities representing the final goal were replaced with that representing the immediate goal.

Attention and Working memory

Associative learning requires attention (Fitts and Posner, 1967). After the rats learned the task and reached an autonomous stage, the skill became relatively automatic and effortless. The neural circuit finished the association by reorganizing its neural responses and settled down to a new steady state. The involvement of attention was reduced accordingly. The results of the experiment tested my hypothesis that the coincidence of spike trains at the learning stage is

stronger than that at the learned stage. The attention might be the major factor contributing to the modulation of the coincidence measurement. In my experiment, attention is needed right after cue on.

The relationship between neuronal synchronization and attention is also reported by other scientists. In a study about the correlations between pairs of neurons, Steinmetz and Roy (Steinmetz et al., 2000; Roy et al., 2007) demonstrated that shifting the focus of attention from a visual to a tactile task alters synchronous firing in SII cortex. Fries (Fries et al., 2002) designed an experiment for monkeys performing a task that depended on location specific visual attention. Their results revealed that more attentional efforts correspond with an increased local synchronization.

Working memory is a theoretical concept central to neuroscience (Baddeley, 2010). Many studies have provided evidence that the prefrontal cortex participates in the process of the temporary storage of information (Goldman-Rakic, 1987; D'Esposito et al., 1995; Rao, 1997). When a short delay is imposed between a cue and a behavioral response, neurons in the prefrontal cortex collectively sustain activity over the memory delay (Miller et al., 1996; Warden and Miller, 2010). Such "delay activity" is thought to play a major role in the temporary memory maintenance (Pribram et al., 1952; Goldman-Rakic, 1990).

In my experiment, we designed the task for the rats to learn the strategy of moving the position of the lights by pressing the control paddles. In the course of directional choice learning, rats formed a strategy by comparing the outcomes from previous trials stored in working memory with their decisions. The demand for the working memory is analogous to the "delay-and-match" task (Rothe et al., 2009). Also, the formation of associations during learning reduces the number of preliminary alternative decisions to account for, and thus the load on information processing. Accordingly, the actual load on working memory further depends on the level of maturation of a behavioral strategy during learning. Stark showed that working memory is critically involved in the

initial formation of associations for new behavioral strategies, i.e. learning (Stark et al., 2008). He showed that there is an increase of working memory activity during the learning process of a complex discrimination task (Stark et al., 2004).

Correlated spike firing plays a critical role in working memory. Neuronal synchronization in the frontal cortex has been reported to occur in a delayed matching-to-sample task which was used to evaluate working memory (Aertsen et al., 1991). In another delayed matching-to-sample experiment, Tallon-Baudry (Tallon-Baudry, 2004) revealed the relationship between the successful performance of a visual short-term memory task and the strength of oscillatory synchrony during the maintenance of the object in short-term memory. Villa and Fuster (Villa and Fuster, 1992) have demonstrated that working memory information can be encoded in temporal structures of spike trains. Sakurai (Sakurai and Takahashi, 2006) designed two working memory tasks and revealed that closely neighboring neurons have dynamic and sharp synchrony modulation to represent certain tasks. Palva (Palva et al., 2010) has observed that neural synchrony was stable and sustained throughout the visual working memory retention period and the synchrony was strengthened with an increasing in memory load.

Conclusion

In this study, by using a rat model performing a directional choice learning task, we showed that the coincidence measurement was the highest when the rats were performing the designed task at the learning stage. The changes in the coincidence measurement may be caused by internal coordination of spike timing, which was not dependent on the explicit presentation of stimulus but more likely to be associated with the implicit cognitive processes. This systematic process suggested the neural coincidence may not be a trivial reflection of anatomical connectivity such as shared input through bifurcating axons but a functionally and internally generated synchronization resulting from dynamic interactions within the cortical network. It also suggested that the precise synchronization of individual action potentials play an important role in

reorganizing AGm and AGl circuits during a directional choice learning process and may encode the information of animal's internal states including attention and working memory.

REFERENCES

Abbott LF, Dayan P (1999) The effect of correlated variability on the accuracy of a population code. Neural Computation 11:91–101.

Abeles M (1991) Corticonics: Neural Circuits of the Cerebral Cortex. Cambridge, UK: Cambridge University Press.

Aertsen A, Vaadia E, Abeles M, Ahissar E, Bergman H, Karmon B, Lavner Y, Margalit E, Nelken I, Rotter S (1991) Neural interactions in the frontal cortex of a behaving monkey: signs of dependence on stimulus context and behavioral state. J Hirnforsch 32:735–743.

Aertsen AM, Gerstein GL, Habib MK, Palm G (1989) Dynamics of neuronal firing correlation: modulation of “effective connectivity”. Journal of Neurophysiology 61:900–917.

Aldworth ZN, Dimitrov AG, Cummins GI, Gedeon T, Miller JP (2011) Temporal Encoding in a Nervous System. PLoS Computational Biology 7:19.

Averbeck BB, Latham PE, Pouget A (2006) Neural correlations, population coding and computation. Nature Reviews Neuroscience 7:358–366.

Baddeley A (2010) Working memory. Current Biology 20:136–140.

Barch DM, Braver TS, Nystrom LE, Forman SD, Noll DC, Cohen JD (1997) Dissociating working memory from task difficulty in human prefrontal cortex. Neuropsychologia 35:1373–1380.

Brenner N, Strong SP, Koberle R, Bialek W, De Ruyter Van Steveninck RR (2000) Synergy in a neural code. Neural Computation 12:1531–1552.

Brown VJ, Bowman EM (2002) Rodent models of prefrontal cortical function. Trends in Neurosciences 25:340–343.

Debarnot U, Clerget E, Olivier E (2011) Role of the Primary Motor Cortex in the Early Boost in Performance Following Mental Imagery Training. PLoS ONE 6:e26717.

Von Der Malsburg C (1981) The Correlation Theory of Brain Function. In: Internal report, pp.R1–R26. Department of Neurobiology, Max Planck Institute for Biophysical Chemistry.

D’Esposito M, Detre JA, Alsop DC, Shin RK, Atlas S, Grossman M (1995) The neural basis of the central executive system of working memory. Nature 378:279–281.

Eagleman D (2007) 10 unsolved mysteries of the brain. Discover 2007:1–6.

Fitts PM, Posner MI (1967) Human performance (Walker EL, ed). Brooks/Cole.

Fries P, Roelfsema PR, Engel AK, König P, Singer W (1997) Synchronization of oscillatory responses in visual cortex correlates with perception in interocular rivalry. Proceedings of the National Academy of Sciences of the United States of America 94:12699–12704.

Fries P, Schroder JH, Roelfsema PR, Singer W, Engel AK (2002) Oscillatory neuronal synchronization in primary visual cortex as a correlate of stimulus selection. Journal of Neuroscience 22:3739–3754.

Goldman-Rakic PS (1987) Circuitry of primate prefrontal cortex and regulation of behavior by representational knowledge. In: Handbook of Physiology (Plum F, Mountcastle V, eds), pp.373–417. American Physiological Society.

Goldman-Rakic PS (1990) Cellular and circuit basis of working memory in prefrontal cortex of nonhuman primates. Progress in Brain Research 85:325–326.

Gray CM, Singer W (1989) Stimulus-specific neuronal oscillations in orientation columns of cat visual cortex. Proceedings of the National Academy of Sciences of the United States of America 86:1698–1702.

Grün S (2009) Data-Driven Significance Estimation for Precise Spike Correlation. Journal of Neurophysiology 101:1126–1140.

Hallett M (1995) the role of the motor cortex in motor learning. Neural Plasticity:89–95.

Hanakawa T (2002) The Role of Rostral Brodmann Area 6 in Mental-operation Tasks: an Integrative Neuroimaging Approach. Cerebral Cortex 12:1157–1170.

Havenith MN, Zemmar A, Yu S, Baudrexel SM, Singer W, Nikolić D (2009) Measuring sub-millisecond delays in spiking activity with millisecond time-bins. Neuroscience Letters 450:296–300.

Heidbreder C (2003) The medial prefrontal cortex in the rat: evidence for a dorso-ventral distinction based upon functional and anatomical characteristics. Neuroscience Biobehavioral Reviews 27:555–579.

Jackson PL, Decety J (2004) Motor cognition: a new paradigm to study self-other interactions. Current Opinion in Neurobiology 14:259–263.

Jones MW (2002) A comparative review of rodent prefrontal cortex and working memory. Current Molecular Medicine 2:639–647.

Kahneman D (1973) Attention and effort. Englewood Cliffs, New Jersey: Prentice-Hall.

Kilavik BE, Roux S, Ponce-Alvarez A, Confais J, Grün S, Riehle A (2009) Long-term modifications in motor cortical dynamics induced by intensive practice. Journal of Neuroscience 29:12653–12663.

Kolb B, Robbins T (2003) The rodent prefrontal cortex. Behavioural Brain Research 146:1–2.

Kouneiher F, Charron S, Koechlin E (2009) Motivation and cognitive control in the human prefrontal cortex. Nature Neuroscience 12:939–945.

De La Rocha J, Doiron B, Shea-Brown E, Josić K, Reyes A (2007) Correlation between neural spike trains increases with firing rate. Nature 448:802–806.

Larkum ME, Zhu JJ, Sakmann B (1999) A new cellular mechanism for coupling inputs arriving at different cortical layers. Nature 398:338–341.

Di Lorenzo PM, Chen J-Y, Victor JD (2009) Quality time: representation of a multidimensional sensory domain through temporal coding. Journal of Neuroscience 29:9227–9238.

Miller EK, Erickson CA, Desimone R (1996) Neural mechanisms of visual working memory in prefrontal cortex of the macaque. Journal of Neuroscience 16:5154–5167.

Milner PM (1974) A model for visual shape recognition. Psychological review 81:521–535.

Mushiake H, Inase M, Tanji J (1991) Neuronal activity in the primate premotor, supplementary, and precentral motor cortex during visually guided and internally determined sequential movements. Journal of Neurophysiology 66:705–718.

Palva JM, Monto S, Kulashekhar S, Palva S (2010) Neuronal synchrony reveals working memory networks and predicts individual memory capacity. Proceedings of the National Academy of Sciences of the United States of America 107:7580–7585.

Paxinos G, Watson C (2007) The rat brain in stereotaxic coordinates, 6th ed. Burington, MA: Elsevier Academic Press.

Pillow JW, Shlens J, Paninski L, Sher A, Litke AM, Chichilnisky EJ, Simoncelli EP (2008) Spatio-temporal correlations and visual signalling in a complete neuronal population. Nature 454:995–999.

Preuss TM (1995) Do Rats Have Prefrontal Cortex? The Rose-Woolsey-Akert Program Reconsidered. Journal of Cognitive Neuroscience 7:1–24.

Pribram KH, Mishkin M, Rosvold HE, Kaplan SJ (1952) Effects on delayed-response performance of lesions of dorsolateral and ventromedial frontal cortex of baboons. Journal of comparative and physiological psychology 45:565–575.

Raichle ME (2010) Two views of brain function. Trends in cognitive sciences 14:180–190.

Rao SC (1997) Integration of What and Where in the Primate Prefrontal Cortex. Science 276:821–824.

Riehle a. (1997) Spike Synchronization and Rate Modulation Differentially Involved in Motor Cortical Function. Science 278:1950–1953.

Rolls ET, Treves A (1998) Neural networks and brain function. New York, NY: Oxford University Press.

Rothe T, Deliano M, Scheich H, Stark H (2009) Segregation of task-relevant conditioned stimuli from background stimuli by associative learning. Brain Research 1297:143–159.

Roy A, Steinmetz PN, Hsiao SS, Johnson KO, Niebur E (2007) Synchrony: a neural correlate of somatosensory attention. Journal of Neurophysiology 98:1645–1661.

Sakamoto K, Mushiake H, Saito N, Aihara K, Yano M, Tanji J (2008) Discharge Synchrony during the Transition of Behavioral Goal Representations Encoded by Discharge Rates of Prefrontal Neurons. Cerebral Cortex 18:2036–2045.

Sakurai Y, Takahashi S (2006) Dynamic synchrony of firing in the monkey prefrontal cortex during working-memory tasks. Journal of Neuroscience 26:10141–10153.

Sanes JN, Donoghue JP (2000) Plasticity and primary motor cortex. Annual Review of Neuroscience 23:393–415.

Seamans JK, Lapish CC, Durstewitz D (2008) Comparing the prefrontal cortex of rats and primates: insights from electrophysiology. Neurotoxicity Research 14:249–262.

Shadlen MN, Movshon J a (1999) Synchrony unbound: a critical evaluation of the temporal binding hypothesis. Neuron 24:67–77, 111–125.

Shannon CE (1948) A Mathematical Theory of Communication. Bell System Technical Journal 27:379–423.

Shima K, Tanji J (1998) Both supplementary and presupplementary motor areas are crucial for the temporal organization of multiple movements. Journal of Neurophysiology 80:3247–3260.

Sillito AM, Jones HE, Gerstein GL, West DC (1994) Feature-linked synchronization of thalamic relay cell firing induced by feedback from the visual cortex. Nature 369:479–482.

Singer W (1999) Neuronal synchrony: a versatile code for the definition of relations. Neuron 24:49–65, 111–125.

Stark H, Rothe T, Deliano M, Scheich H (2008) Dynamics of cortical theta activity correlates with stages of auditory avoidance strategy formation in a shuttle-box. Neuroscience 151:467–475.

Stark H, Rothe T, Wagner T, Scheich H (2004) Learning a new behavioral strategy in the shuttle-box increases prefrontal dopamine. Neuroscience 126:21–29.

Steinmetz PN, Roy A, Fitzgerald PJ, Hsiao SS, Johnson KO (2000) Attention modulates synchronized neuronal firing in primate somatosensory cortex. Nature 404:187–190.

Tallon-Baudry C (2004) Attention and awareness in synchrony. Trends in Cognitive Sciences 8:523–525.

Tsakiris M, Jeannerod M (2008) Motor cognition: What actions tell the self (Oxford Psychology Series, no. 42). Experimental Psychology formerly Zeitschrift für Experimentelle Psychologie 55:212–213.

Tsujimoto S, Genovesio A, Wise SP (2008) Transient neuronal correlations underlying goal selection and maintenance in prefrontal cortex. Cerebral Cortex 18:2748–2761.

Uhlhaas PJ, Pipa G, Lima B, Melloni L, Neuenschwander S, Nikolic D, Singer W (2009) Neural synchrony in cortical networks: history, concept and current status. Frontiers in Integrative Neuroscience 3:17.

Uylings HBM, Groenewegen HJ, Kolb B (2003) Do rats have a prefrontal cortex? Behavioural Brain Research 146:3–17.

Vaadia E, Haalman I, Abeles M, Bergman H, Prut Y, Slovin H, Aertsen A (1995) Dynamics of neuronal interactions in monkey cortex in relation to behavioural events. Nature 373:515–518.

Victor JD, Purpura KP (1996) Nature and precision of temporal coding in visual cortex: a metric-space analysis. Journal of Neurophysiology 76:1310–1326.

Villa AE, Fuster JM (1992) Temporal correlates of information processing during visual short-term memory. NeuroReport 3:113–116.

Wang X-jing (2010) Neurophysiological and Computational Principles of Cortical Rhythms in Cognition. Physiological Reviews 90:1195–1268.

Warden MR, Miller EK (2010) Task-dependent changes in short-term memory in the prefrontal cortex. Journal of Neuroscience 30:15801–15810.

Yang C, Olson B, Si J (2011) A multiscale correlation of wavelet coefficients approach to spike detection. Neural computation 23:215–250.

Yang Y, Raine A (2009) Prefrontal structural and functional brain imaging findings in antisocial, violent, and psychopathic individuals: a meta-analysis. Psychiatry Res Author Manuscript 174:81–88.

Yuste R, MacLean JN, Smith J, Lansner A (2005) The cortex as a central pattern generator. Nature Reviews Neuroscience 6:477–483.

BIOGRAPHICAL SKETCH

Bing Cheng is currently studying Electrical Engineering in the School of Electrical, Computer and Energy Engineering at Arizona State University. In May 2014, he will graduate with an Master of Science degree, with a focus in signal processing and control systems. Mr. Cheng is a member of a number of professional and student organizations including Society for Neuroscience (SFN), Institute of Electrical and Electronics Engineers (IEEE), Tau Beta Pi and Eta Kappa Nu. During the past two years, Bing participated in engineering internships with the Canon Group and Shutterfly Inc. These experiences provided him with valuable experience and insight. Bing has been the recipient of numerous honors and awards including the Pamela & Jack Saltich Fellowship and Shutterfly Scholarship. Bing has presented his research at international conference of Neuroscience. His thesis, Emerging Neural Coincidences in Rats Agranular Medial and Agranular Lateral Cortices During Learning of a Directional Choice Task, was supervised by Dr. Jennie Si. Outside of academics, Bing is very involved in University activities such as Life Among Nations, Friends of Internationals and Graduate Christian Fellowship. He enjoys outside activities including hiking, skiing, fishing and swimming.
38